Three Dimensional Modeling of the Hydrodynamics of Oblique Droplet-Hot Wall Interactions During the Reflood Phase After a LOCA

D. Chatzikyriakou
e-mail: d.chatzikiriakou@imperial.ac.uk

S. P. Walker

B. Belhouachi

Department of Mechanical Engineering,
Imperial College London,
Exhibition Road,
London SW7 2AZ, UK

C. Narayanan

D. Lakehal

ASCOMP GmbH,
Technoparkstrasse 1,
8005 Zurich, Switzerland

G. F. Hewitt
Department of Chemical Engineering and
Chemical Technology,
Imperial College,
Prince Consort Road,
London SW7 2BY, UK

*During the reflood phase, following a loss-of-coolant-accident (LOCA), the main mechanism for the precursory cooling of the fuel is by convective heat transfer to the vapor, with the vapor being cooled by the evaporation of the entrained saturated droplets. However, it is believed that the droplets that reach the rod could have an effect on this cooling process. Despite the fact that those droplets do not actually wet the fuel rod due to the formation of a vapor film that sustains them and prevents them from touching the wall, the temperature drop caused by the impingement of such water droplets on a very hot solid surface (whose temperature is beyond the Leidenfrost temperature (1966, "A Track About Some Qualities of Common Water," Int. J. Heat Mass Transfer, **9**, pp. 1153–1166)) is of the order of 30–150°C (2008, The Role of Entrained Droplets in Precursory Cooling During PWR Post-LOCA Reflood, TOPSAFE, Dubrovnik, Croatia, 1995, "Heat Transfer During Liquid Contact on Superheated Surfaces," ASME J. Heat Transfer, **117**, pp. 693–697). The associated heat flux is of the order of 10^5–10^7 W/m^2 and the heat extracted is in the range of 0.05 J over the time period of the interaction (a few ms) (2008, The Role of Entrained Droplets in Precursory Cooling During PWR Post-LOCA Reflood, TOPSAFE, Dubrovnik, Croatia, 1995, "Heat Transfer During Liquid Contact on Superheated Surfaces," ASME J. Heat Transfer, **117**, pp. 693–697). The hydrodynamic behavior of the droplets upon impingement is reported to affect the heat transfer effectiveness of the droplets. In the dispersed flow regime the droplets are more likely to impinge on the hot surface at a very small angle sliding along the solid wall, still without actually touching it, and remaining in a close proximity for a much larger time period. This changes the heat transfer behavior of the droplet. Here, we investigate numerically the hydrodynamics of the impingement of such droplets on a hot solid surface at various incident angles and various velocities of approach. For our simulations, we use a computational fluid dynamics (CFD), finite-volume computational algorithm (TransAT©). The level set method is used for the tracking of the interface. We present three-dimensional results of those impinging droplets. The validation of our simulation is done against experimental data already available in the literature. Then, we compare the findings of those results with previous correlations.* [DOI: 10.1115/1.4000867]

1 Introduction

The phenomenon of the impingement of liquid droplets onto superheated surfaces is of great importance in many industrial applications. One occasion when the cooling of a hot surface by impingement of water droplets is important is the recovery process ("reflood") following a postulated loss-of-coolant-accident (LOCA) in a pressurized water nuclear reactor (PWR). Then, the fuel elements have risen in temperature (600–900°C). Water is introduced from the bottom (emergency core cooling system) and a two-phase mixture of water and vapor starts rising up the fuel rods. Above this rewetting front, liquid is present in the form of a liquid core, swept upwards by the vapor flow, which breaks up in a complex way to form drops. Cooling of the fuel by this droplet-steam mixture above the rewetting front ("precursory cooling") is vitally important in the reflood process. In this region, the conditions are characterized by the flow of superheated vapor between even hotter metal surfaces, with a population of small droplets entrained in the vapor flow. It is important to understand the mechanisms by which droplets interact with hot surfaces, and this is the focus of the work described here.

Ultimately, the question that both this and the subsequent studies would like to answer is whether those droplets could provide a significant augmentation of the cooling process. More specifically, when a droplet bounces from a hot solid surface, heat is transferred from the solid to the liquid and vapor phases. This both increases the droplet mean temperature (if it is subcooled) and evaporates liquid from the droplet. If the heat transfer rate is large enough during the impact, liquid vaporized from the droplet forms a vapor layer between the liquid and the solid surface [1], which prevents direct contact of the droplet with the surface. In this case, heat transfer is obstructed significantly.

In the dispersed flow regime characterizing reflood, the droplets are likely to impinge on the hot surface at a very small angle, sliding along the solid wall, still without actually touching it, and remaining in a close proximity for a much larger time period than in the case of a perpendicular approach.

The processes accompanying the interaction of a droplet with a

Contributed by the Nuclear Division of ASME for publication in the JOURNAL OF ENGINEERING FOR GAS TURBINES AND POWER. Manuscript received July 29, 2009; final manuscript received August 4, 2009; published online July 7, 2010. Editor: Dilip R. Ballal.

hot surface (spreading, recoiling, bouncing, and evaporating) are complicated, and depend on a number of parameters such as the droplet size, the droplet impact velocity, and the angle at which the droplet approaches the surface. In order to characterize the behavior of the droplets under such circumstances, understanding of phenomena, such as the momentum change, the heat transfer between the droplet and the solid surface, and the residence time of the droplet, has to be gained. Such studies have so far been focused on normal and near-normal approaches. There has been little work on the very shallow approaches that are most relevant to reflood.

Modern CFD techniques offer the ability to model a two-phase flow, accounting explicitly for exchanges in mass, momentum, and energy between the phases. In this study, we use CFD modeling to examine the interaction of droplets with hot solid surfaces at different angles. In particular, we will attempt to validate such a level set CFD model for this purpose, (by comparison with existent measurements and correlations) and then use it to extend this CFD study to the cases of very shallow approaches.

In Sec. 2, a review of previous experimental and computational work in this field is presented. In Sec. 3, the computational model and schemes used for this study are described. The results of our computational study are presented in Sec. 4, and in Sec. 5, we give some concluding remarks.

2 Literature Review

There have been a number of experimental studies on the dynamics of droplets impinging on a solid surface, whose temperature is higher than the Leidenfrost temperature. It has been shown experimentally [2] that the approach velocity of the droplet influences significantly the heat transfer. When the approach velocity increases, then heat transfer increases. That was also shown analytically [3]. The heat loss caused by one droplet would increase with an increase in the perpendicular droplet velocity component. It was shown experimentally [4–7] that in order to evaluate the effect of the droplet size, the velocity and the angle of approach on the impact dynamics (spreading, residence time, angle of rebound, disintegration), the Weber number ($\rho V^2 2R/\sigma$), based on the perpendicular component of the velocity of the droplet, should be considered. In fact, this number is used in the present study. There is a critical value of this number above which the droplet disintegrates upon impingement. That number was found to be around 80 for droplets impinging at 30 deg on a hot plate [4].

The effect of the impact angle on the droplet impact behavior was also studied experimentally [6,8]. It was found that when the angle of impact was 60 deg, then the behavior similar to that of a normal impact was observed, though with more disintegration of the droplet occurring. When the impact angle was changed to 30 deg, no disintegration was observed due to lower impact momentum in the normal direction. It was also shown experimentally [9] that for large angles of impingement, the critical Weber number was of the order of 50. This, however, did not seem to hold for small impingement angles. Then, the critical Weber number was demonstrated to be in the range of 20–30. Above these values, disintegration of the droplets was observed upon impingement and a different heat transfer mechanism would be activated.

Numerical approaches for the beyond Leidenfrost regime employed mostly the volume of fluid (VOF) method ([10–12]) and the level set (LS) method. For interactions of droplets with hot surfaces exceeding the Leidenfrost threshold, both a free slip boundary condition with a contact angle of 180 deg [10] and a no-slip (spreading phase) and free slip boundary condition (recoiling phase) [13] were employed. In those approaches, the effects of the evaporation and the vapor flow were neglected, and a simplified temperature field was assumed. A three-dimensional simulation of a droplet impacting onto a hot flat surface in the Leidenfrost regime using the level set method in a finite-volume algorithm with the arbitrary Lagrangian–Eulerian (ALE) technique was adopted [14,15]. Recently, the present authors used the level set method to reproduce the behavior of a nonwetting droplet, taking into account the evaporation at the bottom of the droplet, as well as surface tension effects [16].

3 Computational Model

3.1 Physical Model. In the present computational work, the dynamic interaction of a droplet with a hot substrate at different angles is simulated. In the present version, evaporative mass transfer from the droplet to the vapor is not accounted for. The energy equation is not solved; heat transfer within the droplet or vapor is not modeled. The vapor boundary layer between the droplet and the hot surface when the droplet is in close proximity to the wall is accounted for by means of a boundary condition that prevents the droplet from touching the wall. This approach is valid for the cases of droplet impingement on solid surfaces sustained at beyond Leidenfrost temperatures. The droplet then does not touch the hot surface due to the existence of a vapor film. The microflow in that layer is studied by the "exact" solution of the flow equations; no empirical "vapor layer model" is used. The droplet is assumed to be spherical at the beginning of the simulation, and the fluids comprising the computational domain (liquid and gas) are treated as incompressible and immiscible.

3.2 Numerical Method

3.2.1 TransAT© Code. We employ the computational multifluid dynamics (CMFD) code TransAT© developed at ASCOMP GmbH, Zurich, Switzerland. This is a multiphysics finite-volume code based on solving multifluid Navier–Stokes equations. The code uses structured meshes, though it allows for multiple blocks to be set together. The grid arrangement is collocated. The solver is pressure based (projection type), corrected using the Karki–Patankar technique for compressible flows (up to transonic flows). High-order time marching and convection schemes can be employed, and up to third-order monotone schemes in space. Multiphase flows are tackled using interface tracking techniques for both laminar and turbulent flows. The one-fluid formulation context on which TransAT© is built is such that the two-phase flow is represented as the flow of a single fluid having physical properties, which vary according to a "color function" advected by the flow. This allows identification of the local phase (gas or liquid). Either the level set or the volume-of-fluid interface tracking methods (ITM) can be employed in the code to track evolving interfaces. In the present work, the level set method was employed.

3.2.2 Droplet Surface Tracking Method. Capturing the interface between the droplet and the surrounding gas involves the use of an interface tracking method appropriate for fixed Eulerian grids. Here, the level set method [17] is being employed. The main advantage of this method is the inherent ability to handle topological changes in a straightforward way. It has been proven to be very reliable in the simulation of curvature-dependent problems such as interface breaking and merging. Here, the level set function ϕ is used in order to separate the liquid and the gaseous phases. The free surface of the droplet is designated by the set of points, where $\phi=0$. Generally, in the computational domain, the level set function is defined as follows:

$$\begin{aligned} \phi(\boldsymbol{x},t) > 0 \quad &\text{for } \boldsymbol{x} \text{ in the liquid phase} \\ \phi(\boldsymbol{x},t) < 0 \quad &\text{for } \boldsymbol{x} \text{ in the gas phase} \\ \phi(\boldsymbol{x},t) = 0 \quad &\text{for } \boldsymbol{x} \text{ at the interface} \end{aligned} \tag{1}$$

The motion of the interface moving with velocity is captured by evolving the level set equation (a Hamilton–Jacobi type convection equation) in the computational domain

$$\frac{\partial \phi}{\partial t} + u_j \frac{\partial \phi}{\partial x_j} = 0 \tag{2}$$

The entire computational domain can be treated as a single domain, and the regions of different materials can be distinguished using the level set function. The density and the viscosity of the whole fluid change continuously from one phase to the other, and are defined as:

$$\rho(\phi) = \rho_g + (\rho_l - \rho_g) H(\phi) \tag{3}$$

$$\mu(\phi) = \mu_g + (\mu_l - \mu_g) H(\phi) \tag{4}$$

where the subscripts l and g denote the liquid and the gas phase, respectively, and $H(\phi)$ is a (smoothed) heaviside function defined as follows (where ε is the interface thickness):

$$H(\phi) = \begin{cases} 0 & \text{if } \phi < -\varepsilon \\ \frac{1}{2}\left[1 + \frac{\phi}{\varepsilon} + \frac{1}{\pi}\sin\left(\pi\frac{\phi}{\varepsilon}\right)\right] & \text{if } |\phi| \le \varepsilon \\ 1 & \text{if } \phi > \varepsilon \end{cases} \tag{5}$$

Numerical diffusion causes the interface to smear around the interface after a single advection stage, which in practice means that the level set ceases to indicate the phase of the fluid reliably. To restore the correct behavior near the interface, an iterative redistancing procedure is performed. During this process, the level set function ϕ is set to be equal to a distance function d that is defined as the signed distance function from a given point in the computational domain to the interface between the two phases. In that context, the following equations have to be integrated to steady state [18]:

$$\frac{\partial d}{\partial \tau} - \mathrm{sgn}(d_o)(1 - |\nabla d|) = 0$$
$$d_o(\boldsymbol{x}, \tau = 0) = \phi(\boldsymbol{x}, t) \tag{6}$$

The redistance function d is actually the level set function ϕ itself at the previous time step

$$d(\boldsymbol{x}, t) = \phi(\boldsymbol{x}, t - \Delta t) \tag{7}$$

Equation (6) is solved after each advection step of Eq. (2), using the nonoscillatory third-order weighted essentially nonoscillatory (WENO) scheme.

3.2.3 Hydrodynamic Model. The equations for viscous incompressible flows that describe the conservation of mass and momentum in a Cartesian coordinate system are

$$\nabla \rho \boldsymbol{u} = 0 \tag{8}$$

$$\frac{\partial \rho \boldsymbol{u}}{\partial t} + \nabla \boldsymbol{u} \cdot \rho \boldsymbol{u} = -\nabla p + \rho \boldsymbol{g} + \nabla(2\mu \tilde{D}) + \sigma \kappa(\phi) \delta(\phi) \nabla \phi \tag{9}$$

where $\boldsymbol{u}$ is the fluid velocity, p is the pressure, ρ is the density, as derived in Eq. (3), μ is the fluid viscosity, as derived in Eq. (4), $\tilde{D}$ is the viscous stresses tensor, σ is the surface tension coefficient, $\delta(\phi)$ is the one-dimensional Dirac delta function, and $\kappa(\phi)$ is the curvature of the free surface calculated by means of the level set function ϕ

$$\kappa(\phi) = \nabla \cdot \frac{\nabla \phi}{|\nabla \phi|} \tag{10}$$

The last term in Eq. (9) represents the surface tension force and is incorporated in the computational modeling as a force that acts only on the computational cells in the vicinity of the free surface. Here, this vicinity is assigned the thickness ε, which is one computational cell. The third-order QUICK scheme is employed to calculate the convective terms of both the Navier–Stokes transport equations and the level set equation, and a third-order Runge–Kutta method is used for the advancing of the time step. Adaptive time-stepping is used choosing the overall time step based on convection, viscosity, surface tension, and gravity.

3.3 Droplet and Vapor Layer Modeling. All simulations here employ a three-dimensional fixed Cartesian grid with nonuniform grid spacing. The grid is refined in the regions of greatest interest: the droplet and the vapor layer below the droplet. The minimum grid spacing in those regions is of the order of 7 μm. Three water droplet diameters are simulated (90 μm, 0.2 mm, and 2 mm), with 18–20 grid points per diameter, respectively. The average time step is around 0.2 μs. The model described is used to simulate submillimetric and millimetric water droplets impinging at different angles on a beyond Leidenfrost temperature surface.

The level set function for water is positive, and for vapor is negative. By imposing negative values in the area below the droplet, where, in reality, vapor is generated, the droplet cannot enter in that region. The fluid properties in that region are inherently updated through the level set function as in the rest of the computational domain.

This specific approach is justifiable in the heat transfer regime that we are considering. Well beyond the Leidenfrost threshold (250°C for water), the droplets do not touch the wall. Instead, they are sustained by a thin vapor layer that has a thickness varying from a few microns to tenths of a millimeter. These vapor layer thickness values were estimated experimentally [4] for large droplets. Here, since we simulate smaller droplet cases as well, we use a smaller vapor layer thickness value. The thickness of that layer is 2 computational cells in every case.

4 Results and Discussion

4.1 Introduction. We now apply these methods to the analysis of droplets bouncing, without wetting, from hot surfaces. Recall that we are here studying only the hydrodynamics of the phenomena, and not the thermal effects and evaporation. To simulate the effect of the layer of vapor formed beneath the droplet by evaporation, we simply force the CFD code to retain a small vapor layer there.

The investigation falls into several stages: We first attempt to provide some validation for the computational approach adopted, by qualitative and quantitative comparison with experimental measurements reported earlier. We then perform a brief parametric study, investigating the effect of the droplet size, and of the angle of approach of the droplet impingement mechanism. Both of these parameters influence the propensity of the droplet to break up during the impact. In Sec. 4.3.3, we gather our computational predictions and compare them with experimental measurements [9].

4.2 Hydrodynamics

4.2.1 Validation. Anders et al. [6] conducted experiments with ethanol droplets impinging on surfaces, whose temperature was above the Leidenfrost temperature, using a high-speed optical camera to observe the droplet behavior during the interaction. Their experiments covered a range of impingement velocities and angles of approach. The measured velocity, before and after the impact, was presented as a function of the Weber number (based on the perpendicular velocity component).

Here, we simulate the same case of droplets in order to provide qualitative validation of our computational model. Then, we use the experimentally measured quantities [6] to compare with the results of our simulations for a wide range of Weber numbers.

4.2.2 Qualitative Comparison. Initially, we compare our simulations with experimental data in a qualitative level. In Fig. 1 we show an indicative case for a medium Weber number (We=7),

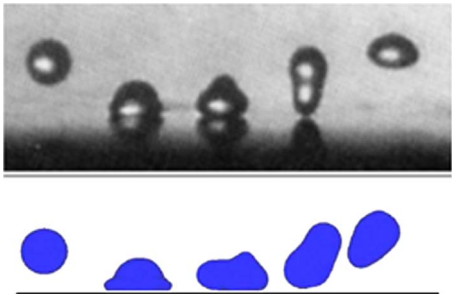

Fig. 1 Qualitative comparison between experimental data [7] and our simulated results (TransAT©). The droplet size is 140 μm and the droplet velocity is 3 m/s. The approach angle is 30 deg. The Weber number here is 7.

where we compare a photographic record with our simulation. The droplet fluid is ethanol and the surrounding gas is air. The predicted behavior matches the observations.

4.2.3 Quantitative Comparison. As shown by Anders et al. [6] (and by numerous other researchers), the droplet velocity component parallel to the wall does not seem to change greatly. Its value after the impact is found to be 0.9–0.95 of its initial value, for all Weber numbers. The perpendicular component of the droplet velocity, however, changes significantly as a result of the interaction. The degree of this change depends on the droplet diameter and the droplet angle of approach. Again, the Weber number can be used to express this dependence. In Fig. 2, we show the dependence on the Weber number of the "before and after" ratio of the droplet perpendicular velocity for both experimental results of Anders et al. [6] and for our simulations.

In our simulations, droplet sizes range from 90 μm to 2 mm, speeds range from 1.2 m/s to 35 m/s, and approach angles from 5 deg to 90 deg. The fluids are ethanol and air.

As shown in Fig. 2, as the Weber number increases to about 15, the fractional reduction in perpendicular velocity increases. This fractional reduction seems to change little with further increase in We beyond ~15. Good agreement between the CFD model and the experimental measurements is observed.

4.3 Parametric Study

4.3.1 Effect of Droplet Size. The droplet size seems to play a vital role in the dynamics of the impact of the droplet with a

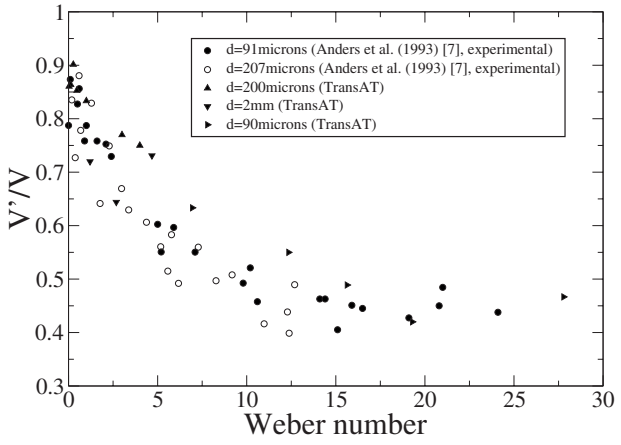

Fig. 2 Ratio of normal droplet velocity component after and before the impact against Weber number. Several droplet sizes and velocities were simulated. Good agreement between the predictions using the TransAT© code and the experimental measurements of Anders et al. [7].

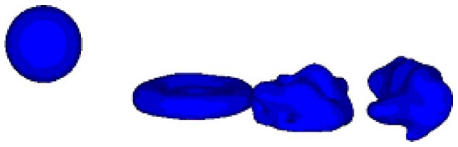

Fig. 3 2 mm drop, angle of approach is 20 deg, initial velocity 1.2 m/s

surface sustained at a temperature higher than the Leidenfrost temperature (beyond Leidenfrost). Big droplets disintegrate more easily, even at a low velocity. Here, (Figs. 3 and 4) we show simulations of a 2 mm and a 200 μm diameter water droplet impinging at 20 deg on a beyond Leidenfrost surface.

The velocity is 1.2 m/s in both cases. The Weber numbers are 0.5 (small drop) and 5 (large drop), respectively. The small droplet retains a broadly spheroidal shape throughout the interaction, while the big droplet spreads and becomes quite convoluted, and seems to be on the verge of breaking-up.

4.3.2 Effect of Angle of Approach. Relatively few experimental data are available in the literature for non-normal interactions, and only one for the very shallow angles likely to be of most interest to reflood.

As suggested by Yao and Cai [9], when small angles of impingement are considered, the tangential velocity component seems to play a vital role in the hydrodynamic behavior of the droplet, and consequently, in the heat transfer mechanism.

The droplet slides along the hot surface for a larger distance, and stays in close proximity for a larger period of time, as the approach becomes more oblique. For a typical case of 200 μm diameter water droplet, the cases of several (fairly large) angles of approach are simulated here (Fig. 5).

Figure 5 shows the behavior for three cases of impact (90 deg, 60 deg, and 20 deg). As is seen, for the 20 deg case, the droplet remains in close proximity to the surface after 8 ms, whereas close

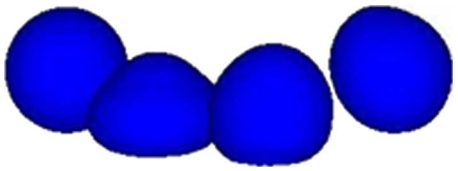

Fig. 4 200 μm drop, angle of approach is 20 deg, initial velocity 1.2 m/s

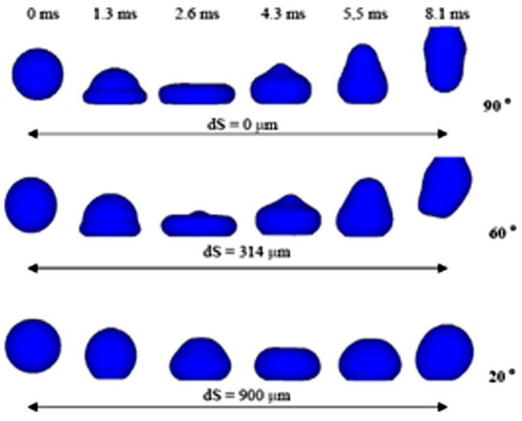

Fig. 5 Simulated results. Water droplets impinging at various angles on a surface beyond the Leidenfrost threshold. The vertical and the 60 deg impact are similar. When small angles of impingement are considered, then the behavior is different. Here, the Weber numbers are 4, 3, and 0.5 from top to bottom. The droplet diameter is 200 μm.

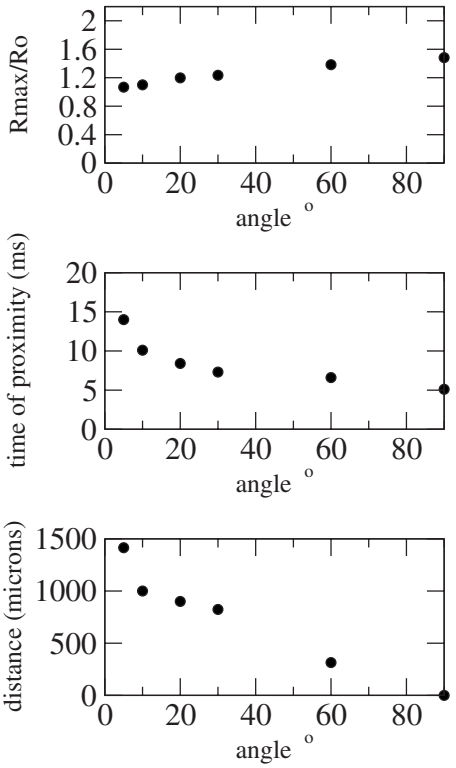

Fig. 6 Spreading of the droplet, time of proximity, and distance it travels close to the wall as a function of angle, for a 200 μm droplet with initial speed 1.2 m/s. These are simulations with TransAT©.

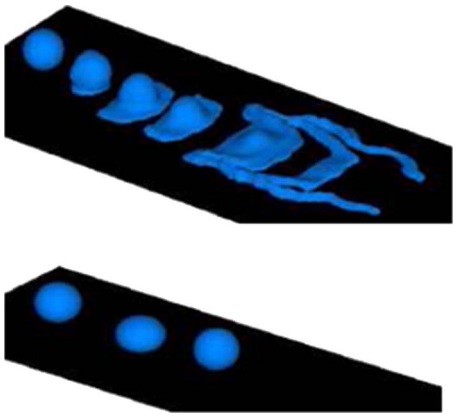

Fig. 7 Upper case: droplet with Weber number equal to 35; lower case: droplet with Weber number equal to 0.3

proximity ceases for the 90 deg and 60 deg cases after 5.5 and 6 ms, respectively.

The time and distance in the direction of travel, during and over which the droplet remains in close proximity to the surface, are shown in more detail in Fig. 6 for a wider range of angles extending down to just 5 deg from the surface for a particular sample drop (200 μm, 1.2 m/s approach speed).

The maximum spreading of the droplet during the interaction, the period of close proximity to the wall, and the distance it travels while close to the wall can be studied effectively only for droplets that do not disintegrate. For droplet breakup cases, the droplet splits into smaller ones and then it is those smaller droplets that need to be studied.

For small angles of impingement, as in the reflood phase, the situation is different and the droplets are expected to impinge on the rod at angles of 5 deg or less. Nevertheless, because of the high axial velocity in the reflood case, these droplets impinge on the hot rod at high Weber numbers.

4.3.3 Droplet Disintegration Upon Impingement. As a final stage to this computational study, we now address the issue of droplet breakup. For a given perpendicular Weber number (as the Weber number is defined and used in this study), it is of course the case that, as the angle of approach becomes more oblique, the droplet speed increases sharply. The energy of the interaction, the shear stresses generated in the thin vapor layer, between the droplet and the plate and the shear stresses between the slow-moving boundary layer vapor and the droplet, are all large. All these factors tend to encourage the breakup of the droplet. This is captured in the simulations, as is seen in Fig. 7, where we see two cases of a 200 μm water droplet in a saturated steam environment approaching the surface at 5 deg with Weber numbers of 35 and 0.3, respectively. The high velocity droplet disintegrates upon impingement, whereas the low energy droplet retains a spherical shape without spreading.

As for perpendicular approaches, there is a critical Weber number above which the droplet disintegrates upon impingement, and this value varies with the angle of approach.

The experimentally generated correlation of Yao and Cai [9] (Eq. (11)) correlates the critical Weber number with the angle of approach, down to the shallow angles of likely interest in reflood. This is shown in Fig. 8

$$\mathrm{We} = 12.89 + 0.85\theta - 0.0053\theta^2 \tag{11}$$

According to that correlation, the smaller the angle of approach is, the smaller the critical (perpendicular) Weber number. For small angles, the tangential velocity component comes into play, as might be expected. In Fig. 8, we plot a series of cases simulated with TransAT© with experimental data [9] about the critical Weber number.

4.3.4 Heat Transfer Estimation. It has been shown through both analytical and experimental studies [3,19] that the amount of heat extracted by a single tiny droplet during the period of its interaction is of the order of 0.05 J. That holds for millimetric droplets impacting vertically or nearly vertically on the hot surface. The time of proximity of the droplet near the wall for such cases (confirmed in the present computations) is of the order of 5–8 ms. However, for nearly horizontal impacts, the time of close proximity of the droplet near the surface increases. Additionally,

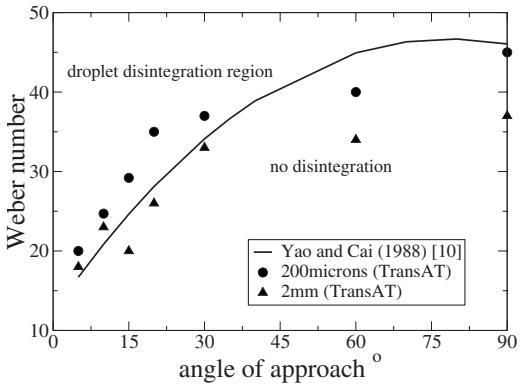

Fig. 8 Effect of angle of approach on the disintegration of the droplet. It is obvious that, for small angles of impingement, the droplet disintegrates at a lower Weber number. Good agreement between experiments and our simulated results.

for high energy impacts, the droplet spreads a lot, covering and consequently cooling a larger area. This could lead to an enhanced heat transfer mechanism.

5 Conclusion

The oblique impact of drops of size smaller than 1 mm may be important in understanding the full range of heat transfer mechanisms during reflood. This has been very little studied to date. In the present work, we have confirmed that modern interface tracking CFD methods are able to reproduce well the hydrodynamic characteristics of these interactions, both for perpendicular and near-perpendicular approaches, and for the practically important case of shallow, oblique approaches.

Having established that the hydrodynamics are well represented, the next step is to incorporate the solution of the energy equation to generate a self consistent model of the entire process. By implementing such a model, it should be possible to obtain a reasonable estimate of the amount of heat transfer during these very brief interactions.

Acknowledgment

This work was carried out as part of the TSEC program KNOO and as such we are grateful to the EPSRC for funding under Grant No. EP/C549465/1.

Nomenclature

Latin Symbols

- d = redistance function
- $\tilde{D}$ = viscous stresses tensor $(1/s)$
- $\boldsymbol{g}$ = gravity $(\mathrm{m/s^2})$
- H = smoothed heaviside function
- p = pressure (Pa)
- R = droplet radius (m)
- $\boldsymbol{V}$ = velocity vector (m/s)
- V = droplet normal velocity component before impact
- V' = droplet normal velocity component after impact
- We = Weber number
- dS = distance traveled by the droplet close to the wall

Greek Symbols

- δ = interface Dirac delta function interface
- ε = thickness of interface
- θ = angle of approach (deg)
- κ = surface curvature $(1/m)$
- μ = absolute viscosity (kg/m s)
- ρ = density $(\mathrm{kg/m^3})$
- σ = surface tension coefficient (N/m)
- τ = pseudo time (s)
- ϕ = level set function

Subscripts/Superscripts

- g = gas
- l = liquid
- o = initial
- max = maximum

References

[1] Leidenfrost, J. G., 1966, "A Track About Some Qualities of Common Water," Int. J. Heat Mass Transfer, **9**, pp. 1153–1166.

[2] Pedersen, C. O., 1970, "An Experimental Study of the Dynamic Behavior and the Heat Transfer Characteristics of Water Droplets Impinging Upon a Heated Surface," Int. J. Heat Mass Transfer, **13**, pp. 369–381.

[3] Chatzikyriakou, D., Walker, S. P., and Hewitt, G. F., 2008, *The Role of Entrained Droplets in Precursory Cooling During PWR Post-LOCA Reflood*, TOPSAFE, Dubrovnik, Croatia.

[4] Wachters, L. H. J., and Westerling, N. A. J., 1966, "The Heat Transfer From a Hot Wall to Impinging Water Drops in the Spheroidal State," Chem. Eng. Sci., **21**, pp. 1047–1056.

[5] Hatta, N., Fujimoto, H., Takuda, H., Kinoshita, K., and Takahashi, O., 1995, "Collision Dynamics of a Water Droplet Impinging on a Rigid Surface Above Leidenfrost Temperature," ISIJ Int., **35**(1), pp. 50–55.

[6] Anders, K., Roth, N., and Frohn, A., 1993, "The Velocity Change of Ethanol Droplets During Collision With a Wall Analysed by Image Processing," Exp. Fluids, **15**, pp. 91–96.

[7] Biance, A.-L., Chevy, F., Clanet, C., Lagubeau, G., and Quere, D., 2006, "On the Elasticity of an Inertial Liquid Shock," J. Fluid Mech., **554**, pp. 47–66.

[8] Kang, B. S., and Lee, D. H., 2000, "On the Dynamic Behaviour of a Liquid Droplet Impacting Upon an Inclined Heated Surface," Exp. Fluids, **29**, pp. 380–387.

[9] Yao, S. C., and Cai, K. Y., 1988, "The Dynamics and Leidenfrost Temperature of Drops Impacting on a Hot Surface at Small Angles," Exp. Therm. Fluid Sci., **1**, pp. 363–371.

[10] Karl, A., Anders, K., Rieber, M., and Frohn, A., 1996, "Deformation of Liquid Droplets During Collisions With Hot Walls: Experimental and Numerical Results," Part. Part. Syst. Charact., **13**, pp. 186–191.

[11] Harvie, D. J. E., and Fletcher, D. F., 2001, "A Hydrodynamic and Thermodynamic Simulation of Droplet Impacts on Hot Surfaces, Part I: Theoretical Model," Int. J. Heat Mass Transfer, **44**, pp. 2633–2642.

[12] Harvie, D. J. E., and Fletcher, D. F., 2001, "A Hydrodynamic and Thermodynamic Simulation of Droplet Impacts on Hot Surfaces, Part II: Validation and Applications," Int. J. Heat Mass Transfer, **44**, pp. 2643–2659.

[13] Fujimoto, H., and Hatta, N., 1996, "Deformation and Rebounding Processes of a Water Droplet Impinging on a Flat Surface Above Leidenfrost Temperature," ASME J. Fluids Eng., **118**, pp. 142–149.

[14] Ge, Y., and Fan, L. S., 2005, "Three-Dimensional Simulation of Impingement of a Liquid Droplet on a Flat Surface in the Leidenfrost Regime," Phys. Fluids, **17**, p. 027104.

[15] Ge, Y., and Fan, L. S., 2006, "3-D Modeling of the Dynamics and Heat Transfer Characteristics of Subcooled Droplet Impact on a Surface With Film Boiling," Int. J. Heat Mass Transfer, **49**, pp. 4231–4249.

[16] Chatzikyriakou, D., Walker, S. P., Hewitt, G. F., Narayanan, C., and Lakehal, D., 2009, "Comparison of Measured and Modelled Droplet—Hot Wall Interactions," Appl. Therm. Eng., **29**(7), pp. 1398–1405.

[17] Osher, S. J., and Sethian, J. A., 1988, "Fronts Propagating With Curvature Dependent Speed: Algorithms Based on Hamilton-Jacobi Formulations," J. Comput. Phys., **79**, pp. 12–49.

[18] Sussman, M., Smereka, P., and Osher, S., 1994, "A Level-Set Approach for Computing Solutions to Incompressible Two-Phase Flows," J. Comput. Phys., **114**, pp. 146–159.

[19] Chen, J. C., and Hsu, K. K., 1995, "Heat Transfer During Liquid Contact on Superheated Surfaces," ASME J. Heat Transfer, **117**, pp. 693–697.